J Mater Sci: Mater Electron (2012) 23:2257–2263
DOI 10.1007/s10854-012-0793-7

Mechanism for the formation of low aspect ratio of $La(OH)_3$ nanorods in aqueous solution: thermal and frequency dependent behaviour

P. S. Kohli · Manish Kumar · K. K. Raina · M. L. Singla

Received: 19 April 2012 / Accepted: 6 June 2012 / Published online: 21 June 2012

Abstract $La(OH)_3$ nanorods of length varying between 30 and 50 nm with aspect ratio of 2–5 were synthesized in aqueous solution using hydrazine hydrate in presence of mixture of cationic *N*-cetyl-*N*,*N*,*N*,trimethylammonium bromide (CTAB) and tetra-*n*-butylammonium bromide (TBAB) surfactants. The resultant product was characterized for its morphology and structure using XRD, TEM and FT-IR. Thermal stability studied using TGA indicated good stability. Surfactants in reaction mixture reduces the surface tension of the solution which lowers the energy needed to form a new phase, resulting in the formation of $La(OH)_3$ crystals of anisotropic shape with low aspect ratio. The A.C. conductivity was found to be of the order of nano-seimen (ns), which non-linearly increases with the increase in frequency (10^2–10^6 Hz) The capacitance behaviour was observed in pF in mid frequency region, which can be useful as low loss dielectric material. Nano rods may work as standard materials to monitor conductivity levels in biofluid proteins.

1 Introduction

The behaviour of nano sized materials strongly depends on their size, shape and morphology [1, 2]. Wet chemical methods have been reported for large scale production of nanomaterials. Solution phase synthesis of nanorods/wires of controlled dimensions is still a challenging task as surface energy favours the spherical particle formation [3]. Synthesis of nanomaterials has been reported in which shape, size is controlled during synthesis by either deploying surfactants/polymer as capping agent or using templates. But still low dimension system such as nanocrystals, thin films, short aspect ratio rods are getting enormous attention due to their potential applications in nanoelectronics, photonics, data recording, fuel cells and sensors [4–6].

Lanthanum and its compounds have unique electronic structure and exhibit number of transition modes involving the 4f shell of these atoms/ions. These compounds have shown outstanding catalytic, optical, electrical and magnetic properties [7, 8]. $La(OH)_3$ and La_2O_3 are rare-earth novel compounds which have been synthesized in various morphologies such as nanopowder, nanotubes, nanowires, nanorods and nanobelts using hydrothermal, solvothermal, precipitation and microwave assisted route in both aqueous and non aqueous medium [9–16]. $La(OH)_3$ nanowires synthesized in these processes have dimensions of the order of microns in length and posses a low aspect ratio except a few reports on controlled size nanorods. More over it involves the use of elevated temperature, higher reaction time and strong alkaline solutions. To the best of our knowledge no electrical behaviour study has been reported on these nanorods. In this work we present a facile route for the synthesis of $La(OH)_3$ nanorods of high aspect ratio and have proposed the mechanism for the same. Synthesis was carried out in aqueous medium using $La(NO)_3$ precursor and hydrazine hydrate as reducing agent under mild heating conditions. A mixture of CTAB and TBAB surfactant is used to control aspect ratio for which reaction mechanism has been discussed. A.C. conductance and capacitance of this material was measured in the frequency range

P. S. Kohli · M. Kumar · M. L. Singla (✉)
Material Research Division (Agrionics), Central Scientific Instruments Organisation, CSIR, Chandigarh 160030, India
e-mail: singla_min@yahoo.co.in

K. K. Raina
School of Physics and Material Science, TIET, Patiala, Punjab, India

of 10^2 Hz to 10^6 Hz. The material being di-electric may be used for fabrication of capacitors.

2 Experimental

2.1 Materials

Following chemicals were used without further purification. Lanthanum Nitrate ($La(NO_3)_3{\cdot}6H_2O$), Loba Chemie, M.W = 433.02, monohydrate hydrazine ($N_2H_4{\cdot}H_2O$, 98 %), Rankem M.W. = 50.06, *N*-cetyl-*N*,*N*,*N*,trimethylammonium bromide (CTAB), Loba Chemie M.W. = 364.46, tetra-n-butylammonium bromide (TBAB), Spectrochem M.W. = 322.38, absolute ethanol (C_2H_5OH), Changshu Yanguan Chemicals, China. Throughout this study deionised (DI) water (18.6 Mohm) Millipore was used.

2.2 Synthesis of $La(OH)_3$ nanorods

In a typical procedure, 5 mM of each CTAB (0.1822 g), TBAB (0.1612 g) and $La(NO_3)_3{\cdot}6H_2O$ (0.2165 g) were dissolved together in DI water (100 ml) in a round bottom glass flask. The reaction mixture was homogenized under slow stirring for about 10 min, to avoid foam formation. 1.215 ml of hydrazine hydrate was added rapidly to this reaction mixture under vigorous magnetic stirring. The reaction mixture was kept at 70 °C for about 1 h in order to complete the precipitation. It was kept as such for some time to cool down to room temperature. The residue was separated from precipitation solution through centrifugation process. It was washed several times with DI water to make free from soluble impurities and finally rinsed with ethanol. The left out precipitation was dried under vacuum at 40 °C.

2.3 Analytical measurements

X-ray diffraction (XRD) patterns were determined with A Panalytical's X'Pert Pro powder X-ray diffractometer using Cu Kα radiation (λ = 1.5406 Å) from a sealed tube operated at 30 kV and 40 mA. Transmission electron microscopy (TEM) studies were carried out using a Hitachi H-7500 operated at an accelerating voltage of 120 kV. The samples for TEM image were prepared by drop-casting the dispersed particles solution on a carbon coated copper grid. For Thermogravimetric Analysis (TGA/DSC; universal V4.1D TA instruments) was used. Mass change variations of the powered sample were recorded in the temperature range of ambient to 1,000 °C in nitrogen atmosphere, at the heating rate of 5 °C min^{-1}. A Fourier transformation infrared (FT-IR) spectrum was recorded on Perkin Elmer RX-1FTIR spectrophotometer in frequency ranging from 500 to 4000 cm^{-1}. The spectra were taken in KBr powder in the form of pellets. Frequency dependence of this material was studied using HIOKI 13530-50 LCR Hi TESTER. All measurement were carried out under vacuum at room temperature, at constant operating voltage (5 V) in the frequency range of 10^2–10^6 Hz. Compressed pellets of 10 mm diameter were made using in house fabricated metal die system under hydraulic pressure of 5 tone load. Electrical contacts were made with silver paste coating at both opposite sides of the pellets.

3 Results and discussion

3.1 XRD analysis

From the XRD pattern (Fig. 1), it is clear that the product obtained is a pure crystalline compound of $La(OH)_3$ phase with hexagonal crystal structure. All diffraction peaks can be indexed as hexagonal $La(OH)_3$ with lattice constants a = 6.5286 Å, c = 3.8588 Å which belongs to $P6_{3/m}$ space group. Typical reflections were found to match JCPDS—international centre for diffraction data for sample code 36-1481. No peak could be attributed to the existence of any other impurity or of La_2O_3. The average crystalline size of as synthesised product was calculated using Debye–Scherrer formula:

$$a = 0.9\lambda/\beta\cos\theta$$

where a, λ, β, and θ are the average crystalline size, Cu–Kα wavelength of X-ray beam (0.1545 nm), full width at half maxima intensity (FWHM) of each peak in Radian and Bragg's diffraction angle respectively was found to be 8 nm from the average value of various reflection peaks, however for the most intense peak corresponding to (111) plane, it is to be 7 nm. Mazloumi et al. [13] observed average crystalline size between 50 and 65 nm, when synthesis was carried out in various alkaline solution where as in another study [9] size was reported to be fine when

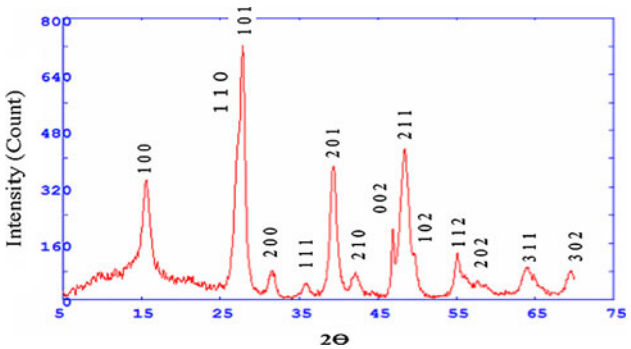

Fig. 1 XRD pattern of $La(OH)_3$ nanorods

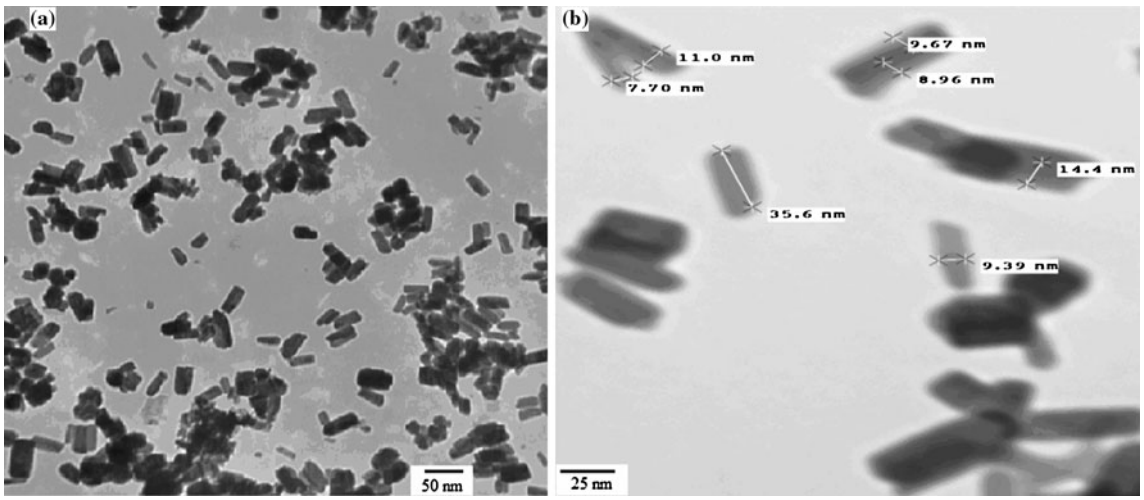

Fig. 2 **a** TEM micrographs of $La(OH)_3$ nanorods, **b** TEM measurements of selected are displaying length and width of nanorods in nm

synthesis was carried out by hydrothermal method in KOH without the use of any surfactant. The broadening of diffraction peaks in the present study clearly indicates the fine crystalline size, which is due to controlled growth of nanocrystals in presence of mixture of surfactant.

3.2 Transmission electron microscope analysis

Figure 2 shows typical TEM image of $La(OH)_3$ nanorods which clearly shows monodisperse nature of anisotropic nanorods with 7–12 nm in width and 30–50 nm in length. These are uniformly dispersed when viewed at different portions of the grid sample. Few rods are appearing as overlapping or in contacting each other, where as at some places only top surface of the rod is visible. From the image, it is clear that there is no agglomeration. The small size and monodispersivity could be attributed to the presence of CTAB/TBAB system in the reaction mixture. Short chain TBA^+ ions function as filler through hydrophobic interactions between alkyl chains of CTAB and butyl chain of TBAB in the gaps of adsorbed long chain CTAB micelles and hence further stabilized nano materials by preventing irregular growth in such gaps [17–19].

3.3 IR analysis

Adsorption behaviour of the surfactant molecules on nano rods surface was observed by taking FT-IR spectra in 4,000–500 cm^{-1} (Fig. 3). For pure CTAB/TBAB symmetric and asymmetric peaks were reported at 2,914.0 and 2,864.0 cm^{-1} and C–H scissoring vibration of N–R moiety were reported at 1,550.0 and 1,474.0 cm^{-1} [17, 20]. In the present study CH_2 stretching vibration lies at 2,924.0 cm^{-1} and 2,850.0 cm^{-1} indicating almost no shift in the head groups of the surfactant molecules. The N–C–H scissoring vibration of N–R has shown a peak at 1,628.2 cm^{-1} which is a significant shift in comparison to pure surfactant molecule. However, a peak at 1,475.7 cm^{-1} indicates the presence of free surfactant CTAB molecule remained trapped inside the product [21]. Also peak appeared at 1,119.2 cm^{-1} is due to –C–N stretching from CTAB molecule have significantly shifted than pure CTAB molecules because adsorption of surfactant molecule. The peak at 1,383.2 cm^{-1} can be attributed to $–CH_3$ bending vibration of tertiary butyl of surfactant TBAB [17]. The bands at 3,426.9 and 1,628.2 cm^{-1} may be due to physiosorbed water molecules. A broad peak at 655.9 cm^{-1} clearly indicates L–OH deformation. This study shows that anisotropic rod formation may be due to the capping behaviour surfactant molecules.

3.4 Thermogravimetric study

TGA/DSC plot of the product in the temperature range of ambient to 1000 °C is given in Fig. 4a. The profile indicates the corresponding weight loss in various temperature range which is divided in four steps, (1) in the temperature range of ambient 199.66 °C. The weight loss of 6.572 % is due to physiosorbed water molecules as well as unbounded CTAB/TBAB molecules. In FT-IR spectra (Fig. 3) the broad band at 3,426.9 and 1,628.2 cm^{-1} due to stretching vibration of physiosorbed water molecules also confirms the presence of water moiety. A peak at 1,457.7 cm^{-1} also confirms the presence of free CTAB as reported [21] (2) further gradual weight loss of 9.673 % in the temperature range 263.23 °C is due to the decomposition of the bounded surfactant molecules into C, H and N moiety. Both CTAB/TBAB were got adsorbed on the surface of the nanorods during synthesis. (3) on further ramping in the temperature range from 263.23 to 649.16 °C the weight loss of 10.66 % was observed due to dehydration of

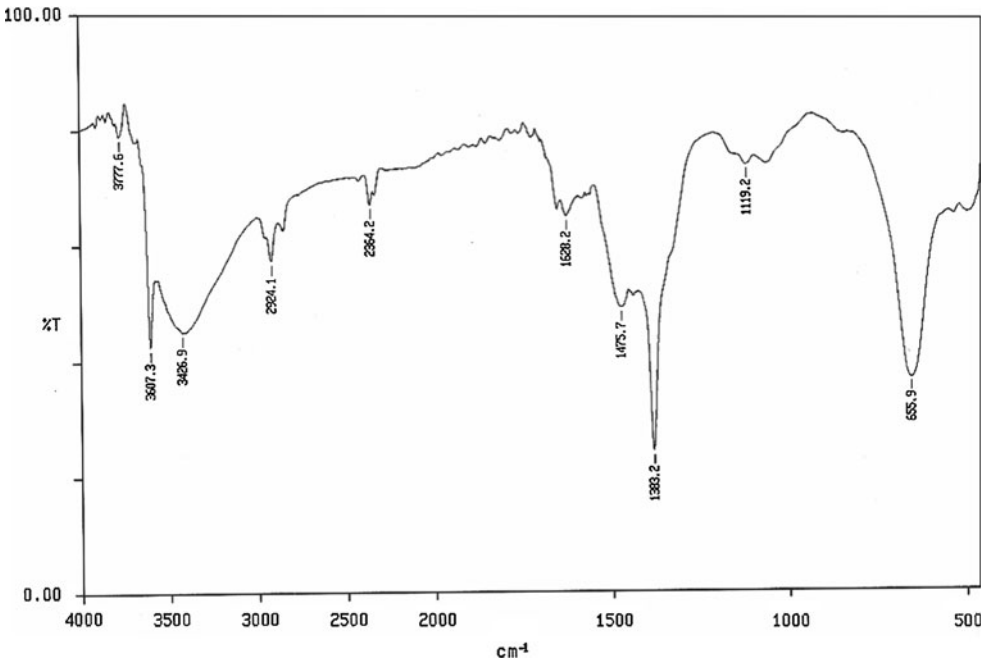

Fig. 3 FT-IR spectra of $La(OH)_3$ nanorods

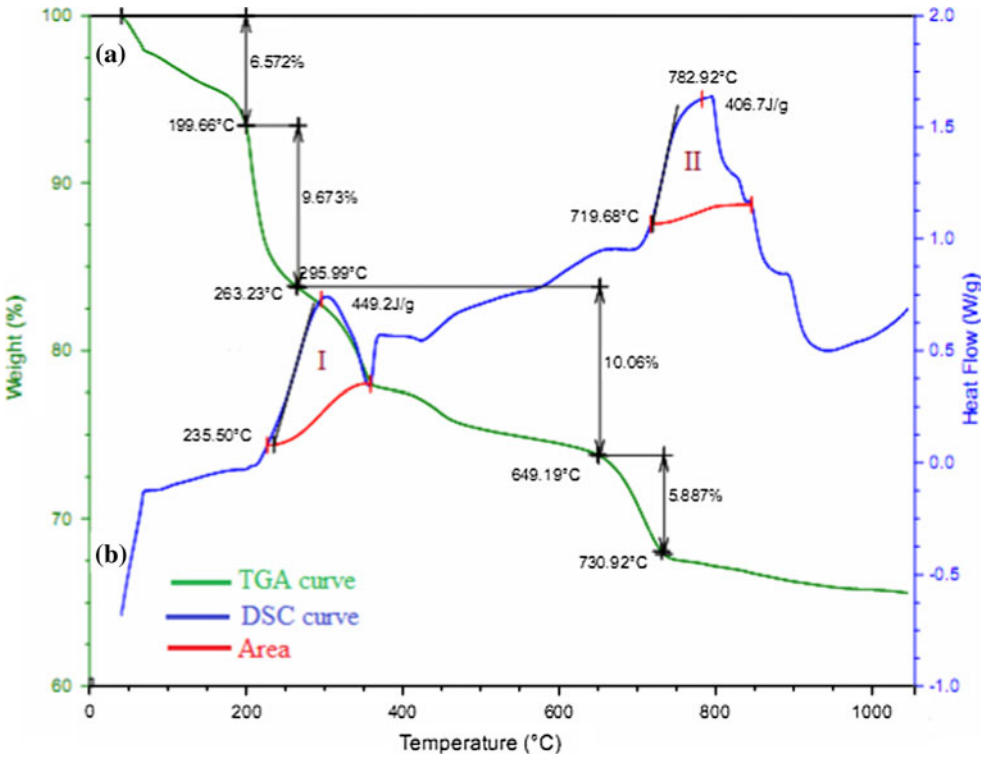

Fig. 4 Thermogravimetric analysis of $La(OH)_3$ nanorods, **b** DSC plot of $La(OH)_3$ nanorods

$La(OH)_3$ to LaOOH (lanthanum hydroxide—oxide) [22]. (4) another weight loss of 5.88 % up to the temperature of 730.92 °C was due to complete dehydration of LaOOH into La_2O_3. It has already been reported that the $La(OH)_3$ phase first get transformed to the LaOOH phase in the temperature range of 330–400 °C which is an intermediate phase with monoclinic crystal structure and P21/m (No.11) space group. It further gets dehydrate form La_2O_3 up to 600 °C as per Eqs. (1) and (2) [22, 23]. However, in the present study there is a possibility that both reaction (1) and (2) may be occurring simultaneously and clear cut distinction may not be possible.

$$2La(OH)_3 \rightarrow 2LaOOH + 2H_2O \quad (1)$$

$$2LaOOH \rightarrow La_2O_3 + H_2O \quad (2)$$

According to Eqs. (1) and (2), the total thermal transformation weigh loss for the conversion of $La(OH)_3$ to La_2O_3 theoretically should be should 13.4 %, which is somewhat higher in the present stud and the decomposition temperature of $La(OH)_3$ to La_2O_3 ranges in the temperature range of 330–730 °C. In the present study the shift in dehydration temperature may be the result of surface modification of particles due to CTAB/TBAB capping.

In DSC curve (Fig. 4b) two endothermic peaks were observed. First peak temperature is 295.99 °C having area 449.2 J/g amounting $\sim$85.3 kJ mol^{-1}. This reaction enthalpy change is due to first dehydration (transformation of $La(OH)_3$ to LaOOH) and is in agreement with the results reported by Neumann and Walter [22]. The second peak temperature at 782.92 °C having peak area 406.7 J/g corresponds to 77.0 kJ mol^{-1} which is due to transformation of LaOOH to La_2O_3. The second reaction enthalpy is higher than already reported [22] may be due to rigid and an isotropic nature of the compound form.

3.5 Frequency dependent electrical study

Figure 5a and b shows the variation in electrical connectivity of the material in the frequency ranging from 10^2 to 10^6 Hz and Table 1 comprises of capacitance and conductance values with respect to variable frequency range selected for the study. The A.C. conductivity was measured in ns, which non-linearly increases with the increase in frequency. Total conductivity of the system is given by

$$\sigma = \sigma_0(T) + \sigma(\omega, T) \quad (3)$$

Here, the first term is dc conductivity which is independent of frequency. The second term is A.C. conductivity may be due to auto ionisation or polarization which occurred due to electro negativity difference between the lanthanum and hydroxyl groups resulting in hopping between metal ions under the effect of electric field. It may also be possible that some of free La^{+3} ions left entrapped inside the crystal structure during the synthesis process which may generate defects in the $La(OH)_3$ crystal. Electron transfer experiments in these materials involve the transfer of charge from one end to another end but no net flow of charge or associated current in between contacts or molecules. However more detailed study is needed to understand proper mechanism. It has observed that capacitance values first decreases sharply at lower frequency and then slowly and becomes nearly constant as shown in Fig. 5b. The capacitive behaviour may be due to space charge polarisation from inhomogeneous dielectric structure. Inhomogeneous structure may be due to nanopore defects in the crystal but exact cause is not clear. This type of electrical behaviour may be useful for designing low loss dielectric capacitors and sensors for monitoring and comparing the conductivity levels of bio-fluids.

Table 1 Capactiance and conductance data of $La(OH)_3$ nanomaterial in the selected frequency range of 0.1–1000 KHz

Frequency (Kilo Hz)	Capacitance (pF)	Conductance (nS)
0.1	142.432	1.2204
0.5	123.53	41
1	116.63	75.055
10	103.65	83.17
50	91.335	1437.7
100	86.995	3212.7
500	78.148	19,990
1,000	75.558	38,600

4 Mechanism of formation

Surfactant assisted synthesis is considered an effective methodology for shape controlled synthesis in nanomaterials

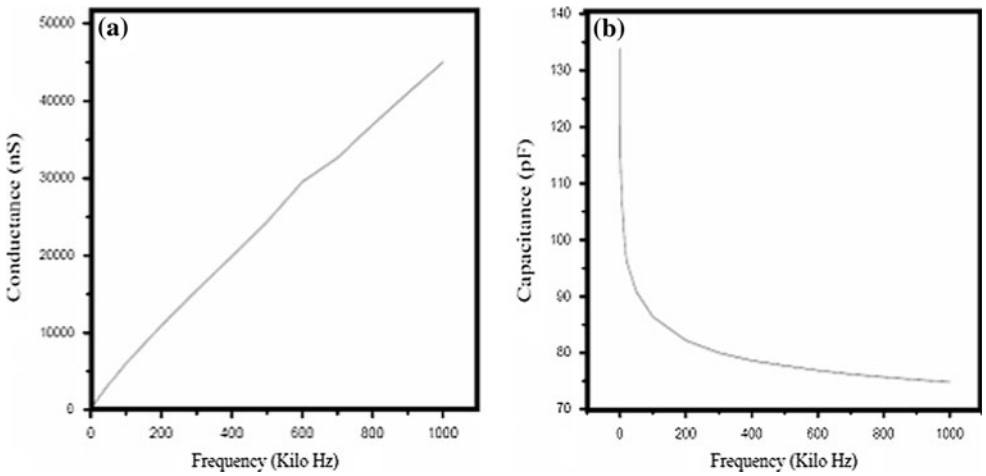

Fig. 5 Frequency dependent electrical study **a** A.C. Conductance versus frequency, **b** Capacitance versus frequency plot of $La(OH)_3$ nanorods in pellet form

in aqueous phase [24, 25]. Hydrazine hydrate is freely soluble in water but since N_2H_4 is basic, chemically free active ions are normally $N_2H_5^+$ and OH^- as per Eq. (4). Lanthanum ions in aqueous solution quickly react with hydroxyl ion to form lanthanum hydroxide due to electrostatic interactions. However presence of excess hot water, the formation of complex co-ordinate complex of $La(OH)_4^{-1}$ occurs which immediately stabilized by the cationic group of surfactants molecules present in the reaction mixture. This reaction product acted as seeding crystal for the transformation into short anisotropic rods of $La(OH)_3$.

$$N_2H_4 + H_2O \leftrightarrow N_2H_5^+ + OH^- \quad (4)$$

Growth process of $La(OH)_3$ rods/crystal in presence of CTAB/TBAB is different than the reaction system having no surfactants. A highly surface active blocks some of the crystal plane because of its preferential adsorption there by directing overall growth in specific direction. Surfactants in reaction mixture reduces the surface tension of the solution which lowers the energy needed to form a new phase, resulting in the formation of $La(OH)_3$ crystals in a lower super saturation [26]. Both CTAB and TBAB are ionic compounds and completely soluble in aqueous medium. The resultant ions are positively charged tetrahedron with a long hydrophobic chain in case of CTAB and short butyl chains with TBAB. Growth unit for $La(OH)_3$ crystal is considered as $La(OH)_4^{-1}$ which have tetrahedron geometry, but negatively charged [27]. Thus $La(OH)_4^{-1}$ and cation CTA^+ forms ion pair due to electrostatic interactions. The complementary between these ion pairs is to provide the surfactant the capability to act as ionic carrier [28]. The Lanthanum particles are negatively charged and CTA^+ got adsorbed on the surface to form a film. The film is floatable which acts as seeding source for assembly and growth of regular crystal structure in the form of rods. In the growth process the surfactant molecule serves as a growth controller as well as agglomeration inhibitor by the forming a covering film on the $La(OH)_3$ rods. These seed crystals will become the nucleating centres and the surfactant molecule carrying the growing unit will be adsorbed on the seed surface. This lending process occurs on the surface of $La(OH)_3$ (0001). As the surfactant forms the film and the molecule will be perpendicularly adsorbed on the surface. It has been earlier studied that the presence of CTAB alone in the reaction mixture has resulted in formation of long fibres with unsymmetrical growth. However, the addition of TBAB restricts the faster longitudinal growth to some extent, because of short butyl groups which possess large hydrophobic volume. TBA^+ ions get mingled in between CTA^+ and both got adsorbed on the top of growing crystal surface. Presence TBAB alone, in the reaction mixture may not be stabilize nano-crystals because of short molecular structure [18]. It may not have stable adherence with another surface and can easily removed on repeated washing. Thus it has been become possible to grow short size anisotropic rods of almost uniform dimensions in presence of the both CTAB and TBAB mixture, more over no alkali hydroxide solution has been deployed in synthesis process.

5 Conclusion

Anisotropic $La(OH)_3$ nanorods have been synthesized through facile route in aqueous medium using a mixture of cationic surfactants in presence of hydrazine hydrate. The morphology indicates narrow size distribution. The growth process CTAB serves as a carrier for $La(OH)_4^{-1}$ and organise the regular structure. TBAB played a key role to limit the growth of nanorods to some extant. Thermal analysis of this material leds to higher stability than pure $La(OH)_3$ crystals grown without surface capping. Repeated A.C. conductance measurements showed conductivity in the level of ns which has also been reported for various bio-fluids hence this material can be utilized to compare A.C. conductance behaviour of such compounds. Due to pF capacitance behaviour, it can be used to build capacitors with low loss.

Acknowledgments The authors are highly thankful to Dr. Pawan Kapur, Director, Central Scientific Instruments Organization (CSIO), Chandigarh for permitted us to carry out research work.

References

1. L.X. Yang, Y. Liang, H. Chen, Y.M. Meng, W. Jiang, Mater. Res. Bull. **44**, 1753 (2009)
2. L. Qiting, N. Jiansen, W. Yiqing, D. Yanan, D. Weizhong, G. Shuhua, J. Rare Earths **29**, 416 (2011)
3. C.J. Murphy, T.K. Sau, A.M. Gole, C.J. Orendorff, J. Gao, L. Gou, S.E. Hunyadi, T. Li, J. Phys. Chem. B **109**, 13857 (2005)
4. X. Duan, Y. Huang, R. Agarwal, C.M. Lieber, Nature **421**, 241 (2003)
5. M.S. Fuhrer, J. Nygard, L. Shih, M. Forero, Y.G. Yoon, M.S.C. Mazzoni, H.J. Choi, Science **288**, 494 (2000)
6. Z.F. Ren, Z.P. Huang, J.W. Xu, J.H. Wang, P. Bush, M.P. Siegal, P.N. Provencio, Science **282**, 1105 (1998)
7. X. Wang, Y. Li, Angew. Chem. Int. Ed. **41**, 4790 (2002)
8. Y.D. Li, Y. Huang, T. Bai, L.Q. Li, Inorg. Chem. **39**, 3418 (2000)
9. X. Ma, H. Zhang, Y. Ji, J. Xu, D. Yang, Mater. Lett. **58**, 1180 (2004)
10. H. Zhang, X. Ma, Y. Ji, J. Xu, D. Yang, Chem. Phys. Lett. **377**, 654 (2003)
11. H. Zhang, Y. Ji, X. Ma, J. Xu, D. Yang, Nanotechnology **14**, 974 (2003)
12. I. Djerdj, G. Garnweitner, D.S. Su, M. Niederberger, J. Solid State Chem. **180**, 2145 (2007)
13. M. Mazloumi, S. Zanganeh, A. Kajbafvala, M.R. Shayegh, D.S.K. Sadrnezhaad, IJE Trans. B: Appl. **21**, 169 (2008)

14. Q. Mu, T. Chen, Y. Wang, Nanotechnology **20**, 345602 (2009)
15. G. Li, C. Li, Z. Xu, Z. Cheng, J. Lin, Cryst. Eng. Comm. **12**, 4208 (2010)
16. F. Bouyer, N. Sanson, M. Destarac, C. Geradin, New J. Chem. **30**, 399 (2006)
17. M.L. Singla, A. Negi, V. Mahajan, K.C. Singh, D.V.S. Jain, Appl. Catal. A-Gen. **323**, 51 (2007)
18. L. Wang, X. Wu, M. Pei, Z. Wu, X. Li, X. Tao, Chinese J. Chem. **29**, 185 (2011)
19. P.S. Kohli, P. Devi, P. Reddy, K.K. Raina, M.L. Singla, J. Mater. Sci.: Mater. Electron. (2012). doi:10.1007/s10854-012-0680-2
20. S.K. Mehta, S. Kumar, S. Chaudhary, K.K. Bhasin, M. Gradzielski, Nanoscale Res. Lett. **4**, 17 (2009)
21. Y. Borodko, L. Jones, H. Lee, H. Frei, G. Somorjai, Langmuir **25**, 6665 (2009)
22. A. Neumann, D. Walter, Thermochim. Acta **445**, 200 (2006)
23. E. Fuglein, D. Walter, Z. Anorg, Allg. Chem. **632**, 2154 (2006)
24. Y. Son, B. Mayers, Y. Xia, Nano Lett. **3**, 675 (2003)
25. F. Kim, K. Sohn, W. Huang, J. Am. Chem. Soc. **130**, 1442 (2008)
26. X.M. Sun, X. Chen, Z.X. Deng, Y.D. Li, Mater. Chem. Phys. **78**, 99 (2002)
27. W.J. Li, E.W. Shi, W.Z. Zhong, Z.W. Yin, J. Crys, Growth **203**, 186 (1999)
28. L. Yan, Y.D. Li, Z.X. Deng, J. Zhuang, X. Sun, Int. J. Inorg. Mater. **3**, 633 (2001)